

Allometric scaling of plant life history

Núria Marbà*, Carlos M. Duarte, and Susana Agustí

Instituto Mediterráneo de Estudios Avanzados, Consejo Superior de Investigaciones Científicas, Universitat de les Illes Balears, Miquel Marqués 21, 07190 Esporles, Spain

Edited by James H. Brown, University of New Mexico, Albuquerque, NM, and approved August 1, 2007 (received for review April 15, 2007)

Plant mortality and birth rates are critical components of plant life history affecting the stability of plant populations and the ecosystems they form. Although allometric theory predicts that both plant birth and mortality rates should be size-dependent, this prediction has not yet been tested across plants ranging the full size spectrum. Here we show that both population mortality and population birth rates scale as the $-1/4$ power and plant lifespan as the $1/4$ power of plant mass across plant species spanning from the tiniest phototrophs to the largest trees. Whereas the controls on plant lifespans are as yet poorly understood, our findings suggest that plant mortality rates have evolved to match population birth rates, thereby helping to maintain plant communities in equilibrium and optimizing plant life histories.

birth | lifespan | mortality | phototrophic organisms | population growth

Plant mortality, the negative loss term in the demographic balance of the populations, has received far less attention than the positive components of plant population dynamics, such as reproductive effort (1, 2). Yet, plant mortality is essential to maintain population turnover and the associated carbon cycling (3). Whereas animal life history has been shown to be closely scaled to body size (4–7), the possible size scaling of plant birth and mortality rates has not yet been tested, despite evidence of a strong size dependence of a range of plant functional traits such as carbon turnover, production, growth, metabolism, and reproduction (2, 8–11).

Plant lifespan varies broadly across phototrophs, from hours in the smallest phytoplankton cells (12) to centuries in large trees (13). These differences suggest a possible size dependence of plant life history, which has been postulated on the basis of theoretical analyses of the optimal plant life history, which predicts plant lifespan (E) to be scaled to the $1/4$ power of individual plant mass (M) (1). This prediction, which is consistent with expectations from the metabolic theory of metabolism predicting specific organismal rates to scale as the $-1/4$ power of size (5–8, 14) and with the $1/4$ power scaling of animal lifespan with body size (4), remains, however, untested. We tested this prediction by examining the scaling of plant birth and mortality rates, lifespan, and population growth with plant mass on the basis of a compilation of published reports yielding 293 and 728 estimates of plant birth and mortality rates, respectively, across the broadest possible range of phototrophic organisms, which span ≈ 6 orders of magnitude in mortality and birth rates, and ≈ 21 orders of magnitude in mass [Table 1 and supporting information (SI) Tables 2 and 3].

Results and Discussion

Plant mortality, D (d^{-1}), was strongly, inversely related to plant mass (grams, dry weight), with mortality rates scaled, as predicted, as the $-1/4$ power of plant mass (Fig. 1). The slope of this relationship is, however, slightly, but significantly, lower than the expected value of $-1/4$ (slope, 95% confidence limit (c.l.) -0.23 to -0.21). Because plant half-life equals $\ln(2)/D$, plant lifespan scales as $M^{0.22}$ (slope, 95% c.l. 0.21 – 0.23), as predicted from optimized life history (1). Organismal birth rate and plant carbon turnover rate have also been reported to scale as $M^{-0.25}$ (5–8).

Our data set confirms that a similar $-1/4$ scaling relationship applies to the scaling of plant birth rate (B , d^{-1}) and M (Fig. 2).

A general balance between plant lifespan and birth rates is required to achieve a balanced population size and density, so that a proportional scaling between plant lifespan and birth rate is expected. Indeed, there was a strong positive scaling between D and B (Fig. 3), but the slope was significantly lower than 1 (slope, 95% c.l. 0.78 – 0.87 ; Fig. 3), indicating that plant birth tended to exceed mortality for the smallest phototrophs. Indeed, the slope of the scaling relationship closely approached, and did not differ significantly from, the expected value of 1 once unicellular phototrophs were excluded from the analysis (slope = 0.94 , 95% c.l. 0.88 – 1.01). Because metabolic theory predicts both birth and mortality to scale as $M^{1/4}$, population growth rate (r = birth – mortality rate) is expected to be size-independent, e.g., M^0 . We tested this prediction by examining the scaling of the ratio of birth to death rates (r , population growth rate) to individual plant mass. Indeed, population growth scaled M^0 (slope = 0.003 , 95% c.l. -0.027 to 0.034) when unicellular phototrophs were excluded from the analysis, demonstrating that all populations (except unicellular phototrophs) were in demographic equilibrium (r = 1) regardless of mass. Phytoplankton cell mortality rates in our data set refer to intrinsic mortality rates, represented by cell lysis, and did not consider mortality due to other removal processes, such as grazing and sinking below the photic layer, which likely remove all of the excess cells, thereby explaining the tendency for phytoplankton birth rates to exceed mortality rates.

The metabolic theory of ecology predicts that metabolic rates should also be temperature-dependent (7, 8). However, the relationship between mortality and birth rates and plant size was independent of temperature in our data set (Student's t test, P = 0.88 and P = 0.21 , respectively), comparable to previous results showing plant functional traits to be more independent of temperature than those of animals (15). The lack of any significant relationship with temperature may be attributable to the large noise in the dependence of mortality and birth rates on plant size, because residual variation involved, on average, a 3-fold variation about the mean value, sufficient to mask any existing relationship with temperature. Indeed, 90% of the mortality reports were derived within a 13°C range (6 – 22°C), for which metabolic theory predicts a 3-fold variability in mortality rates (8), comparable to the residual error of the relationship with mass. There is evidence that mortality rates of phytoplankton (16), macroalgae (17, 18), and land plants (19–

Author contributions: N.M., C.M.D., and S.A. contributed equally to this work, designed research, performed research, analyzed data, and wrote the paper.

The authors declare no conflict of interest.

This article is a PNAS Direct Submission.

Freely available online through the PNAS open access option.

Abbreviations: c.l., confidence limit; dbh, diameter at breast height.

See Commentary on page 15589.

*To whom correspondence should be addressed. E-mail: nuria.marba@uib.es.

This article contains supporting information online at www.pnas.org/cgi/content/full/0703476104/DC1.

© 2007 by The National Academy of Sciences of the USA

Table 1. Mean, standard error, and range (in parentheses) of individual mass, mortality rate, life span, and birth rate across plant types

| Plant type | <i>n</i> | Individual mass, grams dry weight | Mortality rate, d ⁻¹ | Life span, d | Birth rate, d ⁻¹ |
|---------------------------|----------|--|--|---|--|
| Phytoplankton | 48 | 3.5 ± 2.4 × 10 ⁻⁹ (3.4 × 10 ⁻¹⁵ –8.3 × 10 ⁻⁸) | 39 ± 7.0 × 10 ⁻² (1.2 × 10 ⁻³ –2.5) | 2.3 ± 1.2 × 10 ¹ (2.8 × 10 ⁻¹ –5.8 × 10 ²) | 15 ± 2.5 × 10 ⁻¹ (4.0 × 10 ⁻² –3.7) |
| Macroalgae | 37 | 7.2 ± 4.6 × 10 ¹ (7.3 × 10 ⁻⁴ –1.5 × 10 ³) | 7.6 ± 1.8 × 10 ⁻³ (2.2 × 10 ⁻⁴ –5.8 × 10 ⁻²) | 4.0 ± 1.2 × 10 ² (1.2 × 10 ⁻¹ –3.1 × 10 ³) | 1.4 ± 0.63 × 10 ⁻² (2.6 × 10 ⁻⁴ –3.8 × 10 ⁻²) |
| Mosses | 7 | 2.1 ± 0.26 × 10 ⁻² (1.6 × 10 ⁻² –3.3 × 10 ⁻²) | 1.8 ± 0.27 × 10 ⁻³ (6.7 × 10 ⁻⁴ –2.8 × 10 ⁻³) | 4.8 ± 1.0 × 10 ² (2.5 × 10 ² –1.0 × 10 ³) | |
| Ferns | 3 | | 2.6 ± 1.0 × 10 ⁻⁴ (1.3 × 10 ⁻⁴ –4.6 × 10 ⁻⁴) | 3.4 ± 1.1 × 10 ³ (1.5 × 10 ³ –5.2 × 10 ³) | 2.0 ± 0.32 × 10 ⁻⁴ (1.2 × 10 ⁻⁴ –2.8 × 10 ⁻⁴) |
| Seagrasses | 151 | 3.1 ± 0.37 × 10 ⁻¹ (7.0 × 10 ⁻³ –2.5) | 2.5 ± 0 – 35 × 10 ⁻³ (5.6 × 10 ⁻⁵ –4.1 × 10 ⁻²) | 13 ± 1.4 × 10 ² (1.7 × 10 ¹ –1.2 × 10 ⁴) | 1.9 ± 0.20 × 10 ⁻³ (3.9 × 10 ⁻⁵ –1.2 × 10 ⁻²) |
| Land and salt marsh herbs | 190 | 4.9 ± 2.4 (1.8 × 10 ⁻² –1.2 × 10 ²) | 5.8 ± 1.5 × 10 ⁻³ (1.4 × 10 ⁻⁵ –2.2 × 10 ⁻¹) | 16 ± 3.0 × 10 ² (3.2–5.0 × 10 ⁴) | 2.1 ± 0.44 × 10 ⁻³ (1.1 × 10 ⁻⁵ –2.0 × 10 ⁻²) |
| Succulent plants | 12 | 2.9 ± 1.4 × 10 ³ (4.4 × 10 ² –6.1 × 10 ³) | 8.9 ± 2.2 × 10 ⁻³ (2.6 × 10 ⁻⁵ –2.0 × 10 ⁻²) | 7.6 ± 3.3 × 10 ³ (3.5 × 10 ¹ –2.7 × 10 ⁴) | 2.1 ± 0.8 × 10 ⁻⁵ (6.7 × 10 ⁻⁶ –3.6 × 10 ⁻⁵) |
| Shrubs and lianas | 20 | 5.9 ± 3.2 × 10 ¹ (4.5–1.8 × 10 ²) | 1.1 ± 0.6 × 10 ⁻² (1.1 × 10 ⁻⁴ –1.2 × 10 ⁻¹) | 14 ± 4.1 × 10 ² (6.0–6.5 × 10 ³) | |
| Mangroves | 30 | 2.8 ± 1.3 × 10 ¹ (6.4 × 10 ⁻¹ –3.2 × 10 ²) | 3.5 ± 0.94 × 10 ⁻³ (2.4 × 10 ⁻⁵ –2.3 × 10 ⁻²) | 1.8 ± 0.94 × 10 ³ (3.0 × 10 ¹ –2.8 × 10 ⁴) | |
| Trees | 230 | 7.7 ± 1.2 × 10 ⁵ (11–11 × 10 ⁶) | 2.9 ± 0.53 × 10 ⁻⁴ (2.8 × 10 ⁻⁷ –5.2 × 10 ⁻³) | 1.1 ± 0.2 × 10 ⁵ (1.3 × 10 ² –2.5 × 10 ⁶) | 4.1 ± 0.65 × 10 ⁻⁵ (3.0 × 10 ⁻⁶ –3.1 × 10 ⁻⁴) |
| Overall | 728 | 23 ± 4.2 × 10 ⁴ (3.4 × 10 ⁻¹⁵ –11 × 10 ⁶) | 2.9 ± 0.58 × 10 ⁻² (2.8 × 10 ⁻⁷ –2.5) | 37 ± 6.7 × 10 ³ (2.8 × 10 ⁻¹ –2.5 × 10 ⁶) | 1.3 ± 0.32 × 10 ⁻¹ (3.0 × 10 ⁻⁶ –3.7) |

n indicates the number of plant mortality estimates, the variable with the largest number of observations in the data set.

21) increase with increasing temperature. Resolving the temperature-dependence of plant mortality rates, which requires dedicated experimental research, is of fundamental importance in light of the predicted global warming.

Analyses of covariance showed that the allometric scaling between mortality rate and size differed for aquatic and land plants (*t* test, $P < 0.0001$), with a steeper reduction in mortality rate with plant mass ($D \approx M^{-0.32}$) for land than for aquatic plants ($D \approx M^{-0.16}$), whereas no such difference was found for plant birth rate (*t* test, $P > 0.86$). Similarly, the scaling between mortality rate and size differed for vascular and nonvascular plants (Student's *t* test, $P < 0.0001$), with a steeper reduction in

mortality rate with M ($D \approx M^{-0.31}$) for vascular than for nonvascular plants ($D \approx M^{-0.14}$). These differences suggest that differences associated with the aquatic vs. terrestrial and vascular vs. nonvascular contrasts, such as the need for supporting structural materials and possible water stress on land compared with aquatic plants and the requirements to transport solutes for vascular compared with nonvascular plants, may affect mortality rates and plant lifespan.

The controls on organismal death and lifespan remain unclear, and probably include a suite of regulatory processes interacting at various levels, from molecular to organismal, including met-

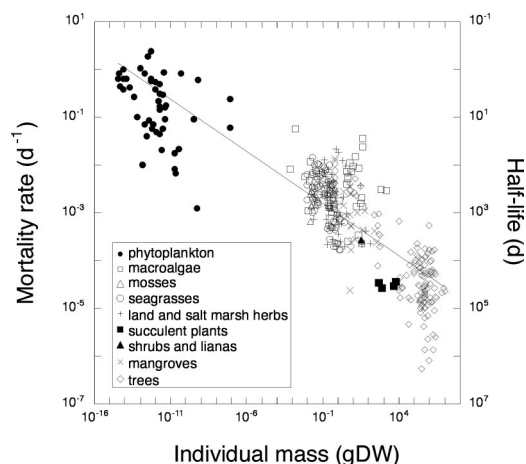


Fig. 1. The relationship between plant mortality rate (D) and the individual mass (M) of plants ranging across phytoplankton, macroalgae, mosses, seagrasses, land and salt marsh herbs, succulent plants, shrubs, lianas, mangroves, and trees. The line shows the fitted regression equation $D = 0.0009 M^{-0.22}$ (slope, 95% c.i. -0.23 to -0.21 , $r^2 = 0.77$, $n = 396$). The corresponding half-life is also indicated in the plot. gDW, grams dry weight.

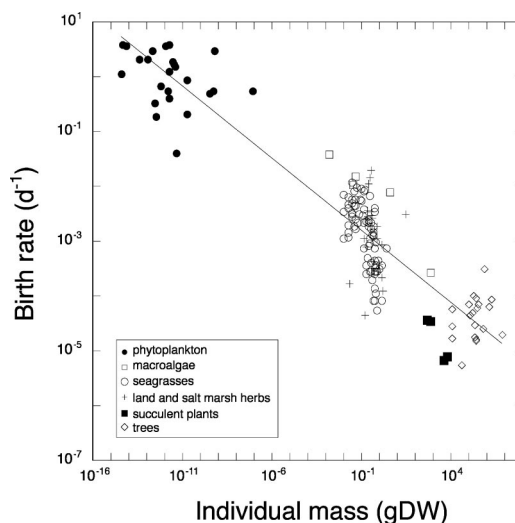


Fig. 2. The relationship between plant birth rate (B) and the individual mass (M) of plants ranging across phytoplankton, macroalgae, seagrasses, land and salt marsh herbs, succulent plants, and trees. The line shows the fitted regression equation $B = 0.0008 M^{-0.27}$ (slope, 95% c.i. -0.28 to -0.24 , $r^2 = 0.84$, $n = 158$). gDW, grams dry weight.

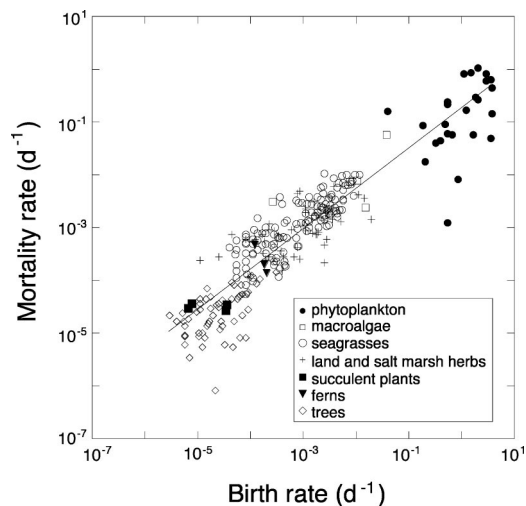


Fig. 3. The relationship between plant mortality (D) and birth (B) rates for plants ranging across phytoplankton, macroalgae, ferns, seagrasses, land and salt marsh herbs, succulent plants, and trees. The line shows the fitted regression equation $D = 0.31 B^{0.82}$ (slope, 95% c.l. 0.78–0.87, $r^2 = 0.84$, $n = 289$).

abolic processes such as imbalanced respiration and production with increasing age, reproduction, structural imbalances in trees, failure and accumulated damage at the cellular level, including the expression of sublethal genes and somatic mutations, and crowding-dependent mortality (22, 23). Whereas the action of selective processes on animal lifespan cannot extend through their entire lifespan because many lose reproductive capacity with age, this is not the case in plants, which generally remain reproductive throughout their lifespan, suggesting that lifespan could be under greater selective pressure in plants. Whatever the nature of the controls, our results suggest that plant lifespan and mortality rates are roughly scaled to birth rates, which is an important requirement to maintain stable populations. The $-1/4$ power scaling of mortality and birth rates with plant size demonstrated here implies that, for a given primary production, communities dominated by small plants will generate a larger flow of detritus from dying organisms than those dominated by larger, long-lived plants, substantiating previous empirical laws relating stand carbon turnover to plant size (8). That plant mortality rate is size-dependent is also consistent with the size dependence of the maximum density of plant stands beyond which crowding-derived mortality operates (24). Crowding, which is strongly size-dependent (24), is known to be a major driver of mortality in plant stands, further supporting the expectation that plant mortality rates should also be size-dependent. Because both mortality and birth rates decline with increasing mass, the demographic equilibrium of large plants requires considerably greater time than that of the smallest plants (e.g., phytoplankton). Although phytoplankton grow much faster than trees, they also die more quickly, accounting for the much smaller biomass they support in both cultured and wild populations compared with that of larger plants.

The results presented here confirm the prediction, derived from the general allometric plant life history model (1), that lifespan and mortality and birth rates should scale as the $1/4$ and $-1/4$ power, respectively, of plant mass, and demonstrate the potential of allometric-based analyses to explain and understand the contrasting life history traits, where the balance between mortality and birth rates play prominent roles, of photosynthetic organisms in the biosphere.

Materials and Methods

Data Compilation. We searched the literature, as well as our own data sets, for reports of plant mortality, birth, and size. We

compiled 694 published and 34 unpublished estimates of mortality rate including estimates for phytoplankton, macroalgae, mosses, ferns, seagrasses, land herbs, salt marsh plants, succulent plants, shrubs, lianas, mangroves, and trees (SI Table 2). When provided, we also compiled estimates on individual mass, height, diameter at breast height (dbh) or biovolume, and birth rate. Individual mass was estimated from individual height by using published allometric relationships between plant height and mass (2). Phytoplankton mass was estimated from biovolume estimates by using published relationships (25). Tree mass (M , in grams dry weight) was estimated from dbh (in centimeters), by using the log-log regression equation fitted for a compilation of an independent data set encompassing the broadest range of size for the tree flora with dbh >4 cm (SI Table 3),

$$M = 78 \cdot \text{dbh}^{2.47}$$

Slope 95% c.l. 2.26–2.71; $R^2 = 0.91$; $N = 49$.

The slope of the fitted equation was not statistically different from $8/3$ (26). Small trees (dbh <4 cm) were excluded from the analysis because $\log M$ scales nonlinearly to $\log \text{dbh}$ (26).

Demographic Parameters for Multicellular Plants. Plant birth and mortality rates of multicellular plants (e.g., macroalgae, mosses, ferns, seagrasses, land herbs, salt marsh plants, succulent plants, shrubs, lianas, mangroves, and trees) were estimated by using individual repeated census (i.e., the appearance of new, untagged plants and the loss of tagged plants in plots of tagged plants, respectively), or derived from the analysis of individual age structure of plant populations. All demographic parameters were measured in field populations. Mortality rate (D , in d^{-1}) was expressed as the exponential rate of decrease of the number of individuals per day. Mortality rate was calculated from the reciprocal individual half-life ($t_{1/2}$, in days) for 3 macroalgae, 1 seagrass, 24 land herbs, 9 shrubs, and 18 tree populations as

$$D = \frac{\ln(2)}{t_{1/2}}$$

Birth rates (B , in d^{-1}) were calculated from the number of individuals at time 0 (N_0) and the number of new-born individuals (N_B) during the time elapsed between individual censuses (t) as

$$B = \frac{\ln(N_0 + N_B) - \ln(N_0)}{t}$$

and from the total number of individuals (N_t) and the number of individuals older than 1 year ($N_{>1}$), assuming that mortality was not different between individuals younger and older than 1 year when birth rate was derived from individual age structure of the population as

$$B = \frac{\ln(N_t) - \ln(N_{>1})}{365}$$

Demographic Parameters for Phytoplankton. Phytoplankton birth rate was calculated as the exponential increase in cell abundance with time for cultured populations. For natural populations, phytoplankton birth rate (d^{-1}) was calculated from measurements of gross carbon production [GP(C)] and phytoplankton carbon [Phyt(C)], assuming daily carbon production to be allocated to increase biomass as described in the equation

$$B = \ln\left(\frac{\text{GP(C)} + \text{Phyt(C)}}{\text{Phyt(C)}}\right)$$

